Author Manuscript

Author Manuscript

Author Manuscript

Author Manuscript

HHS Public Access

Author manuscript

J Bone Miner Res. Author manuscript; available in PMC 2019 May 01.

Published in final edited form as:

J Bone Miner Res. 2018 May ; 33(5): 921–929. doi:10.1002/jbmr.3365.

Bone Tissue Collagen Maturity and Mineral Content Increase With Sustained Hyperglycemia in the KK-Ay Murine Model of Type 2 Diabetes

Heather B Hunt[1], **Jared C Pearl**[1], **David R Diaz**[1], **Karen B King**[2,4], and **Eve Donnelly**[1,3]

[1]Department of Materials Science and Engineering, Cornell University, Ithaca, NY, USA

[2]Department of Orthopedics, University of Colorado School of Medicine, Aurora, CO, USA

[3]Hospital for Special Surgery, New York, NY, USA

[4]Surgical Service/Orthopaedic Service, Veterans Affairs Eastern Colorado Health Care System, Denver. CO, USA

Abstract

Type 2 diabetes mellitus (T2DM) increases fracture risk for a given bone mineral density (BMD), which suggests that T2DM changes bone tissue properties independently of bone mass. In this study, we assessed the effects of hyperglycemia on bone tissue compositional properties, enzymatic collagen crosslinks, and advanced glycation end-products (AGEs) in the KK-Ay murine model of T2DM using Fourier transform infrared (FTIR) imaging and high-performance liquid chromatography (HPLC). Compared to KK-aa littermate controls ($n = 8$), proximal femoral bone tissue of KK-Ay mice ($n = 14$) exhibited increased collagen maturity, increased mineral content, and less heterogeneous mineral properties. AGE accumulation assessed by the concentration of pentosidine, as well as the concentrations of the nonenzymatic crosslinks hydroxylysylpyridinoline (HP) and lysyl pyridinoline (LP), did not differ in the proximal femurs of KK-Ay mice compared to controls. The observed differences in tissue-level compositional properties in the KK-Ay mice are consistent with bone that is older and echo observations of reduced remodeling in T2DM.

Keywords

COLLAGEN: BONE MATRIX; MATRIX MINERALIZATION: BONE MATRIX; GENETIC ANIMAL MODELS: ANIMAL MODELS; OTHER: ANALYSIS/QUANTITATION OF BONE; OTHER: DISEASES AND DISORDERS OF/RELATED TO BONE

Address correspondence to: Eve Donnelly, PhD, Department of Materials Science and Engineering, Cornell University, 227 Bard Hall, Ithaca, NY 14853, USA. eve.donnelly@cornell.edu.

Disclosures

All authors state that they have no conflicts of interest.

Additional Supporting Information may be found in the online version of this article.

Author Manuscript Author Manuscript Author Manuscript Author Manuscript

Introduction

Type 2 diabetes mellitus (T2DM) increases fracture risk for a given bone mineral density (BMD),[1,2] and the greater fracture risk for patients with T2DM persists after adjustment for age, body mass index (BMI), and physical activity.[3] Additionally, T2DM-related fractures are underpredicted by current clinical fracture risk assessment tools that rely heavily on BMD, such as the Fracture Risk Assessment Tool (FRAX).[2] Taken together, these findings suggest T2DM degrades bone quality independently of BMD, which motivates further assessment of bone tissue properties from patients with T2DM.

The precise mechanisms responsible for the putative alterations in bone quality that increase T2DM-related fractures are unknown; however, changes in the posttranslational modifications of collagen due to hyperglycemia have been suggested as a contributing factor. Posttranslational modifications of collagen include (i) crosslinking through enzymatically-mediated processes; and (ii) the formation of a heterogeneous group of reaction products collectively known as advanced glycation end-products (AGEs) through non–enzymatically-induced processes. Enzymatic crosslinking is controlled by the action of lysyl oxidase and results in the formation of trivalent crosslinks such as hydroxylysylpyridinoline (HP, also referred to as pyridinoline) and lysylpyridinoline (LP, also referred to as deoxypyridinoline).[4] Non–enzymatically-induced AGEs, on the other hand, form through the reaction of extracellular reducing sugars (eg, glucose, ribose, fructose) with free amino groups in proteins and can result in nonenzymatic crosslinks, as well as other non-crosslinking AGEs (eg, carboxymethyl-lysine).[5]

Whereas enzymatic crosslinks strengthen and stabilize the collagen matrix,[6] AGEs decrease energy absorption and embrittle bone tissue in animal models,[7] and in glycated/ribosylated human[8] and bovine tissue in vitro.[9] Rodent models supply direct evidence that T2DM impairs whole-bone fracture resistance, and the skeletal phenotypes of rodents with T2DM are typically characterized by substantial reductions in maximum load and inconsistently by reductions in energy to failure and BMD (summarized in Nyman and colleagues[10]). For example, spontaneously diabetic WBN/Kob rats exhibited reduced maximum load and work-to-fracture with no change in BMD compared to controls, and these weakening and embrittlement processes were accompanied by concomitant decreases in enzymatic collagen crosslinks and increases in nonenzymatic collagen crosslinks.[11]

Additionally, AGEs impair bone remodeling processes. In AGE-modified collagen, osteoblastic growth and differentiation were disrupted,[12,13] and apoptosis increased.[14] Observations of reduced bone formation in T2DM patients compared to non–diabetes mellitus (non-DM) controls are also supported by analysis of histomorphometric data[15] and biochemical markers of bone formation.[16–18]

A promising model to study T2DM is the KK-Ay mouse, and to date, compositional skeletal characteristics of the KK-Ay mice have not been evaluated.[19] Mice from the KK strain exhibit insulin insensitivity and glucose intolerance,[20,21] yet they are neither glucosuric nor hyperglycemic.[20,22,23] The addition of the A^y mutation to the KK mouse induces obesity and a distinguishing yellow coat, and KK-Ay mice exhibit overt glucosuria and

Author Manuscript Author Manuscript Author Manuscript Author Manuscript

hyperglycemia around 8 weeks of age.[22,23] When tested in three-point bending, the tibias of KK-Ay mice had a lower ultimate load compared to controls,[24] which may parallel the impaired structural integrity observed in humans.

Prior studies of the skeletal properties of KK-Ay mice compared to controls consistently report reduced trabecular BMD,[24–26] whereas the findings for cortical volumetric BMD (vBMD), total areal bone mineral density (aBMD), and bone formation/resorption markers are less consistent. In two studies comparing KK-Ay mice to C57BL/6 controls, one study reported a decrease in cortical area, thickness, and vBMD with a concomitant decrease in osteoblastogenesis and osteoclastogenesis,[24] and in contrast, the other study reported an increase in cortical thickness and vBMD with an upregulation of osteoblast-related and osteoclast-related gene expression.[25] Although skeletal morphology[24–27] and collagen crosslinks[11,27–29] have been characterized in T2DM bone, compositional data beyond ash weight[30–32] and mineral:matrix ratio (using Raman spectroscopy)[27,32] are limited. These results underscore the need for compartment-specific (ie, trabecular, cortical) and whole-bone compositional assays of T2DM bone tissue.

Therefore, the objective of this work was to compare the spatially-resolved compositional properties and collagen crosslinks of bone tissue from KK-Ay mice with overt T2DM (A^y/a) to their non-overt T2DM siblings (a/a). We hypothesized that hyperglycemia would increase tissue-level nonenzymatic crosslinking (due to AGE accumulation) and would increase tissue mineral content and collagen maturity (due to reduced bone turnover) in the A^y/a mice compared to the a/a controls.

Materials and Methods

Obese mouse model of T2DM

Male KK.Cg-A^y/J mice were purchased from The Jackson Laboratory (Bar Harbor, ME, USA; 002468) at 8 weeks of age, raised in ventilated cages at 20°C to 22°C with a 14-hour light-dark cycle, and given free access to standard irradiated chow (2920x; Harlan Laboratories, Inc., Indianapolis, IN, USA). The yellow heterozygous A^y/a mice were used to model T2DM and their black homozygous a/a littermates were used as controls.

The femurs used here were the nonoperative controls from a study of the effects of T2DM on osteoarthritis progression.[33] At 12 weeks of age, mice within each group (A^y/a: $n = 14$; a/a: $n = 8$) were anesthetized and chosen at random to undergo either a destabilization medial meniscus (DMM) or sham procedure on the left distal femur.[34] The right femurs used in the current study were not operated or otherwise treated. Body masses at the time of surgery were recorded. A minimum of three blood glucose measurements were performed via tail nick test (Precision Xtra Blood Glucose Test Strips; Abbott Diabetes Care Inc., Alameda, CA, USA), with three of the measurement time points at 8 weeks of age (at purchase from Jackson Laboratory), 12 weeks of age (at DMM surgery), and 20 weeks of age (at euthanasia). A lifetime-average blood glucose level (average of all blood glucose measurements for each mouse) greater than 300 mg/dL confirmed hyperglycemic status of the A^y/a mice and euglycemic status of the a/a mice.[19] For a subset of the mice (A^y/a: $n = 4$; a/a: $n = 4$), fasting blood glucose measurements were taken. Because fasting blood

Author Manuscript Author Manuscript Author Manuscript Author Manuscript

glucose in mice may not be representative of steady-state conditions,[35] the blood glucose measurements of these mice were excluded from mean blood glucose calculations for each group. No other treatments were applied to these mice throughout the study. Mice were euthanized with carbon dioxide at 20 weeks of age, and the femurs were dissected. The stifle joints (including the distal half of each femur) were allocated to osteoarthritis analyses,[33] and the proximal halves of the femurs were allocated to bone tissue compositional analyses for the current study. The proximal femurs were wrapped in saline-soaked gauze and frozen at −20°C. All animal care and procedures were performed at the University of Colorado School of Medicine with the approval of the Institutional Animal Care and Use Committee.

Fourier transform infrared imaging

Fourier transform infrared (FTIR) imaging was used to evaluate bone tissue compositional properties in a spatially resolved fashion. The proximal femurs were thawed, dehydrated in graded organic solvents, and embedded in poly(methyl methacrylate) (PMMA). For each of the femurs, three nonconsecutive, 1-μm-thick longitudinal sections spaced a minimum of 10 μm apart were cut near the mid-plane of the femur with a microtome (SM2500; Leica Biosystems, Nussloch, Germany) and placed on BaF_2 windows (Spectral Systems, Hopewell Junction, NY, USA).

FTIR images were collected at two levels of structural hierarchy: (i) a whole-proximal-femur image was generated at 25 μm spatial resolution; and (ii) tissue-specific cortical and trabecular regions of interest (ROIs) (size: 400 μm × 500 μm) were generated at 6.25 μm spatial resolution. For each section, a single whole-proximal-femur image, in addition to three cortical and three trabecular ROIs (Supporting Fig. 1), were collected over the spectral range 800 to 2000 cm^{-1} at a spectral resolution of 4 cm^{-1} using an infrared imaging system (Spotlight 400; Perkin-Elmer Instruments, Waltham, MA, USA). Subsequently, chemical imaging software (ISys; Malvern Instruments, Worcestershire, UK) was used to remove the background, baseline, and subtract the PMMA spectral contribution from the bone spectra.[36] For five proximal femurs, soft tissue on the femoral head was present at the time of PMMA embedding. This soft tissue was excluded from FTIR image analysis with a spectral mask.

For each image, the infrared spectrum at each pixel was analyzed to determine the following parameters: mineral:matrix ratio; carbonate:phosphate ratio; collagen maturity; and mineral crystallinity.[37] The mineral:matrix ratio (area ratio of the phosphate ν_1–ν_3 and amide I peaks) characterizes tissue mineral content[38,39]; the carbonate:phosphate ratio (area ratio of the carbonate ν_2 and phosphate ν_1–ν_3 peaks) characterizes the extent to which carbonate substitutes into the mineral lattice[40]; collagen maturity (the intensity ratio of 1660 cm^{-1} and 1690 cm^{-1}) is related to the ratio of mature, nonreducible collagen crosslinks to immature, reducible collagen crosslinks[41]; and the mineral crystallinity (intensity ratio of 1030 cm^{-1} and 1020 cm^{-1}) is related to crystal size and perfection assessed by X-ray diffraction.[42] Two outcome measurements were obtained for each FTIR parameter from each image: the mean value of all pixels and the distribution width (calculated as the full-width at half-maximum [FWHM] of the Gaussian curve fit to the distribution of pixels; Fig. 2) to assess compositional heterogeneity. Thus, eight outcomes were assessed separately for

Author Manuscript Author Manuscript Author Manuscript Author Manuscript

cortical, trabecular, and whole-proximal-femur ROIs: (i) mean mineral:matrix ratio; (ii) mean carbonate:phosphate ratio; (iii) mean collagen maturity; (iv) mean crystallinity; (v) mineral:matrix ratio FWHM; (vi) carbonate:phosphate ratio FWHM; (vii) collagen maturity FWHM; and (viii) crystallinity FWHM.

High-performance liquid chromatography

High-performance liquid chromatography (HPLC) was used to quantify the AGE pentosidine in the whole proximal femur. The enzymatic crosslinks HP and LP were quantified as secondary outcomes.

Following completion of FTIR imaging, the proximal femurs were de-embedded from PMMA through agitation in methyl acetate for 3 days, with a solution change every 24 hours. After de-embedding, the femurs were agitated in 100% acetone (24 hours), 100% ethanol (24 hours), and isopropyl ether (3×, 15 min). After rinsing with deionized (DI) water, the femurs were lyophilized then hydrolyzed in 6N HCl at 110°C for 18 hours. The hydrolysates were dried in a vacuum centrifuge (Speed Vac SC110A; Savant, Farmingdale, NY, USA) then resuspended in an internal standard solution containing 10nM pyridoxine and 2.4μM homoarginine; 30 μL of internal standard solution was added for every mg of dried bone. The resuspended samples were filtered, then diluted 1:5 with 10% acetonitrile (vol/vol) and 0.5% heptafluorobutyric acid (vol/vol).

Samples were injected into the column and separated using two isocratic steps.[29,43] A calibrator containing all three crosslinks (pentosidine, HP, LP) was serially diluted 1:2 five times to create a linear calibration curve. The pentosidine standard was purchased from Case Western Reserve University (Cleveland, OH, USA), and the HP and LP standards were purchased from Quidel (8004; Quidel, Athens, OH, USA). Separations were performed with a Gemini-NX C-18 column (Phenomenex, Torrance, CA, USA) connected to a programmable HPLC system (Model 126; Beckman Coulter, Inc., Fullerton, CA, USA). 32 Karat Workstation software (version 5.0; Beckman Coulter, Inc., Brea, CA, USA) was used to control the autosampler, pump, and fluorimeter (Model FP1520; Jasco, Easton, MD, USA). Data analysis was performed using 32 Karat Workstation software and MATLAB (2012a, The MathWorks, Inc., Natick, MA, USA).

Pentosidine, HP, and LP concentrations were normalized by collagen concentration as determined by hydroxyproline concentration. For the hydroxyproline measurements, an aliquot of the diluted sample from the crosslink analysis was further diluted 1:50 with 6μM homoarginine in 0.1M borate buffer (pH 11.4), derivatized using 6mM 9-fluorenylmethyl chloroformate for 40 min, and extracted using pentane. Pentane extraction removes excess fluorenylmethyloxycarbonyl chloride (FMOC-Cl) reagent, FMOC-OH reaction product, and acetone. Three extractions were performed, then 25% (vol/vol) acetonitrile in 0.25M boric acid (pH 5.5) was added. The separation of amino acids was run using the same column and system as the crosslink separations using the injection sequence described by Bank and colleagues.[44] Five serial 1:2 dilutions of purified hydroxyproline (Sigma-Aldrich, St. Louis, MO, USA) and 6μM homoarginine in 0.1M borate buffer (pH 11.4) were used to make a linear calibration curve for hydroxyproline. Collagen concentration was determined

Author Manuscript Author Manuscript Author Manuscript Author Manuscript

from the constant ratio of hydroxyproline in fibrillar collagen (300 mol hydroxyproline per mol collagen).

The final outcomes for HPLC included concentrations for pentosidine, HP, and LP. The ratio of HP to LP (HP:LP), the total concentration of mature enzymatic crosslinks (HP+LP), and the ratio of pentosidine to mature enzymatic crosslinks (Pentosidine:HP+LP) were also examined.

Statistical analysis

Mouse characteristics (body mass, lifetime-average nonfasting blood glucose) and collagen crosslinks (pentosidine, HP, LP) were assessed for normality and homogeneity of variances, and a two-tailed Student's *t* test was performed to assess differences between groups. A significance level of 0.05 was used for all analyses.

For the eight FTIR outcome variables, cortical, trabecular, and whole-proximal-femur regions were analyzed separately. For each region, a linear mixed model was used to assess the relationship between genotype (*A^y^/a*, *a/a*) while accounting for the multiple sections analyzed per mouse (three sections/femur) and for repeated measurements made within each section (three trabecular ROIs and three cortical ROIs). To test if the increased mass of the *A^y^/a* mice versus controls had an effect on the FTIR outcome variables, subsequent linear mixed models that included the fixed effect of body mass were analyzed. Pairwise differences between groups were assessed with Tukey post hoc tests. The reported percent differences for FTIR parameters were calculated from the raw data, while the *p* values were determined by the linear mixed models.

The relationships of lifetime-average blood glucose with all FTIR imaging and HPLC outcomes were analyzed to elucidate the effects of hyperglycemia on tissue material properties. Cortical, trabecular, and whole-proximal-femur FTIR ROIs were regressed separately with lifetime-average blood glucose to highlight potential region-specific effects of hyperglycemia. Because AGE accumulation may also affect bone turnover, the relationships of pentosidine and the proximal femur FTIR outcomes were also investigated. The HPLC measurements of collagen crosslinks were performed on the homogenized whole proximal femur, so region-specific (ie, cortical, trabecular) correlations were not assessed between pentosidine and the FTIR imaging outcomes. For all regressions, *A^y^/a* and *a/a* data were pooled because the relationships did not differ between groups ($p > 0.05$).

Results

Mouse characteristics

The *A^y^/a* mice experienced hyperglycemia for a minimum duration of 12 weeks and were heavier than their *a/a* littermate controls. In *A^y^/a* mice relative to controls, the lifetime-average nonfasting blood glucose was 83% higher (mean ± SD; *A^y^/a*: 426.5 ± 49.2 mg/dL versus *a/a*: 234.5 ± 5.1 mg/dL; $p \ll 0.001$), and body mass at time of DMM surgery was 16% higher (A*^y^/a*: 36.7 ± 3.8 g versus *a/a*: 31.5 ± 2.6 g; $p = 0.0024$). Furthermore, hyperglycemia in the *A^y^/a* mice was confirmed over the 12-week study period. The nonfasting blood glucose of the *A^y^/a* mice was 67% greater than the *a/a* mice at 8 weeks of

Author Manuscript Author Manuscript Author Manuscript Author Manuscript

age (A^y/a: 346.2 ± 130.6 mg/dL versus a/a: 207.6 ± 18.5 mg/dL; $p < 0.001$), 114% greater at 12 weeks of age (at DMM surgery): (A^y/a: 413.3 ± 93.2 mg/dL versus a/a: 193.0 ± 11.8 mg/dL; $p < 0.001$), and 76% greater at 20 weeks of age (at euthanasia): (A^y/a: 456.8 ± 76.3 mg/dL versus a/a: 258.5 ± 41.7 mg/dL; $p < 0.001$).

FTIR imaging: parameter distribution means and widths

Bone tissue from the A^y/a mice exhibited greater mean collagen maturity and mineral content, and narrower distribution widths of carbonate:phosphate ratio and crystallinity compared to the a/a mice.

Compared to a/a controls, mean collagen maturity was greater in the A^y/a mice in cortical bone (+12%, $p = 0.0285$; Figs. 1*A*, 2*A*), trabecular bone (+8%, $p = 0.0399$; Figs. 1*A*, 2*C*), and in the whole proximal femur (+7%, $p = 0.0499$; Figs. 1*A*, 2*B*). In the whole proximal femur, the mean mineral:matrix ratio was greater in A^y/a mice compared to controls (+12%, $p = 0.0233$; Figs. 1*A*, 2*D*) and trended toward being greater in cortical bone (+8%, $p = 0.0790$; Fig. 1*A*). Body mass had a significant positive effect on the mean mineral:matrix ratio in cortical bone ($p < 0.001$); however, no observed effect of body mass on mean mineral:matrix ratio was observed in the trabecular or whole proximal femur regions or in the mean collagen maturity of cortical, trabecular, and whole proximal femur regions. The mean carbonate:phosphate ratio and mean crystallinity were similar between A^y/a and a/a mice across all regions. Distributions were narrower in the A^y/a mice compared to controls for carbonate:phosphate ratio (–19%, $p = 0.0078$; Figs. 1*B*, 3*A*) and crystallinity (−24%, $p = 0.0099$; Figs. 1*B*, 3*B*) in the whole proximal femurs. The distribution widths were similar for all other parameters.

HPLC collagen crosslinks

The concentrations of pentosidine, HP, and LP and the parameters HP:LP, HP+LP, and Pentosidine:HP+LP in the whole proximal femur were similar between groups (Table 1).

Association of blood glucose with collagen crosslinks and tissue material properties

When relationships between lifetime-average blood glucose and FTIR imaging parameters were examined, these parameters were correlated in trabecular and whole-proximal-femur ROIs, but not in cortical ROIs. In the trabecular ROIs, lifetime-average blood glucose correlated with (i) carbonate:phosphate ratio FWHM and (ii) collagen maturity FWHM, and (iii) trended toward a correlation with mean collagen maturity (Table 2). In the whole-proximal-femur ROIs, lifetime-average blood glucose correlated with (i) mean collagen maturity, (ii) carbonate:phosphate ratio FWHM, and (iii) crystallinity FWHM, and (iv) trended toward a correlation with mineral:matrix ratio FWHM (Table 2).

Lifetime-average blood glucose did not correlate with the concentrations of pentosidine, HP, and LP assessed by HPLC, or with HP:LP, HP+LP, or Pentosidine:HP+LP (Table 2). The concentration of pentosidine did not correlate with any whole-proximal-femur FTIR imaging parameters; however, pentosidine correlated with (i) HP, (ii) LP, and (iii) HP+LP (Table 2).

Author Manuscript Author Manuscript Author Manuscript Author Manuscript

Discussion

In this study, we assessed the effects of hyperglycemia on bone tissue AGEs and material properties in the KK-Ay murine model of T2DM. The blood glucose levels and body masses of the KK-Ay mice in this study are comparable to previously reported values,[21,23] and confirm the KK-Ay mice to be hyperglycemic and obese. The control mice were euglycemic and overweight.

Our data reveal that bone tissue from *A^y/a* mice has (i) increased collagen maturity, (ii) increased mineral content, and (iii) less heterogeneous mineral properties compared to control *a/a* mice. Specifically, the greater mean collagen maturity, assessed with FTIR imaging observed in *A^y/a* versus *a/a* bone tissue, demonstrates a higher ratio of mature enzymatic crosslinks to immature crosslinks, which is consistent with older, more mature tissue.[41] The greater mean mineral:matrix ratio observed in *A^y/a* versus *a/a* bone tissue similarly points to an increased tissue age (ie, time since tissue formation), because older tissue will have a greater mineral content.[45] The narrower distribution widths of the carbonate:phosphate ratio and crystallinity of *A^y/a* versus *a/a* whole proximal femoral bone tissue suggest the *A^y/a* mice had less bone turnover.[46]

Several key mechanisms can modulate tissue properties in murine bone, even at cortical sites that lack a robust intracortical remodeling process. The observed alterations in mean mineral content may arise from (i) differing rates of periosteal expansion and endosteal resorption[47] or (ii) direct osteocytic regulation.[48] In healthy tissue, changes in collagen maturity typically reflect turnover; however, the alterations in this parameter observed in the KK-Ay mice could alternatively arise from an accelerated rate of conversion from divalent to trivalent enzymatic crosslinks. In the absence of double-labels for new bone formation, the current study design precludes discernment of the precise mechanism(s) responsible for the observed changes in tissue properties. Furthermore, prior findings regarding the balance of formation and resorption markers in KK-Ay mice are in conflict: some studies report decreased bone turnover markers,[24] whereas others report upregulation of bone turnover-related gene expression.[25] Together, these findings indicate complex, compartment-dependent effects of hyperglycemia in the KK-Ay mouse model.

Previous studies of the KK-Ay mouse[25,26] and other rodent models of T2DM[27,32] point to a larger effect of T2DM on BMD in trabecular bone compared to cortical bone and the whole bone. In this study, a greater mean collagen maturity was observed in the bone tissue of *A^y/a* mice versus the *a/a* mice in all compartments examined (trabecular, cortical, and whole proximal femur), but no differences in mineral properties were observed in the trabecular compartment. It is likely that two key factors affected our ability to detect subtle differences in mineral properties in trabecular bone: (i) the small analysis area of trabecular compartments (ie, the number of bone pixels versus non-bone pixels per ROI) and (ii) the inherent variability of the distribution width, particularly in the carbonate:phosphate ratio.

The regressions of FTIR imaging parameters with mean blood glucose support the interpretation that the *A^y/a* tissue is older with less turnover and that the reduced turnover is in part due to hyperglycemia. Mean collagen maturity in trabecular bone and the whole

Author Manuscript Author Manuscript Author Manuscript Author Manuscript

proximal femur increased with worsening hyperglycemia (R^2 = 0.253, p = 0.0669; R^2 = 0.600, p = 0.0300, respectively), and the carbonate:phosphate ratio and crystallinity distribution widths in the whole proximal femur narrowed with increasing hyperglycemia (R^2 = 0.430, p = 0.0150; R^2 = 0.600, p = 0.0300, respectively) (Table 2). Together, these results indicate that the *A^y/a* bone tissue is older, consistent with the observations of disrupted and/or reduced remodeling processes in T2DM.[15–18]

One potential explanation for the greater mineral content observed in the *A^y/a* versus *a/a* mice is body mass. Because the *A^y/a* mice were heavier than the *a/a* controls, the greater tissue mineral content observed in the *A^y/a* mice may reflect an adaptive response. When body mass was added as a factor in the linear mixed models for the mean mineral:matrix ratio and collagen maturity parameters, body mass had a significant positive effect on mean mineral:matrix ratio in the cortical compartment ($p < 0.001$). Thus, it is likely that body mass is a contributing factor for the increased mineral content in the *A^y/a* versus *a/a* mice; however, the lack of an effect of body mass with respect to the collagen maturity indicates body mass alone does not describe the observed changes to the collagen in the *A^y/a* mice.

AGE accumulation in the whole proximal femur assessed by pentosidine concentration did not increase with hyperglycemia in *A^y/a* mice, as shown by the lack of correlation between lifetime-average blood glucose and pentosidine concentration in the whole proximal femur (Table 2). Although bone tissue ribosylated and glycated at supraphysiological concentrations in vitro is characterized by increased total AGEs and pentosidine,[8,9,49,50] evidence of AGE accumulation due to T2DM in vivo is currently inconclusive. Specifically, bone tissue pentosidine concentration increased in T2DM rats compared to non-DM controls[11]; however, no difference in pentosidine concentration was found in a study of human bone from T2DM and non-DM patients.[28]

There are several factors that may explain the similar levels of pentosidine between *A^y/a* and *a/a* mice. First, pentosidine is just one of hundreds of AGE species, and although HPLC measurement of pentosidine concentration is accepted as a sensitive assay of this crosslink, it has not yet known if tissue pentosidine concentration is a representative measurement of all tissue AGE species.[51] Second, cortical and trabecular bone differentially accumulate AGEs, but the differences show inconsistent trends. Human trabecular bone accumulated more fluorescent AGEs than cortical bone during in vitro glycation and ribosylation,[49,50] but cortical bone accumulated more pentosidine than trabecular bone in in vivo studies of type 1 diabetic[52] and nondiabetic women and men.[53] In the current study of the proximal femur, the masses of the murine trabecular and cortical diaphyseal tissue alone were too small to generate detectable signals for HPLC. Consequently, the whole proximal femurs were homogenized for HPLC analyses, thereby preventing analysis of compartment-specific pentosidine accumulation. Because of this limitation, a difference in pentosidine concentration between genotypes in trabecular or cortical bone, which may have been detected in a compartment-specific assay, could have been masked in the homogenized assay by equal (or opposite) concentrations across genotypes in the other compartment. Third, the formation of AGEs like pentosidine can take weeks to form in vivo.[54] It is possible that the 20-week lifespan of these mice was not long enough to accumulate more pentosidine in the *A^y/a* mice compared to *a/a* mice, even in hyperglycemic conditions. To our knowledge, no

Author Manuscript Author Manuscript Author Manuscript Author Manuscript

study monitoring the progression of AGE accumulation with aging in mice has been performed; however, pentosidine concentrations in T2DM rats did not differ from non-DM rats until 12 months of age.[11]

The concentrations of the enzymatic crosslinks HP and LP were similar between groups which indicates that the concentration of mature pyridinoline crosslinks in the whole proximal femur remained constant with hyperglycemia. These results are consistent with data from a T2DM rodent model[11] and T2DM human tissue.[28,29] Although concentrations of immature crosslinks were not assessed directly, the effects of hyperglycemia on their concentrations can be inferred. Because collagen maturity (as measured with FTIR) increased, and HP and LP (as measured with HPLC) did not change in the A^y/a versus a/a mice, the observed increase in collagen maturity may be due to a decrease in enzymatic crosslinking. This effect is consistent with a decrease in immature enzymatic crosslinking observed in T2DM rats.[11]

There are several limitations and strengths to note for interpreting our findings. First, nonfasting blood glucose measurements were only available for approximately two-thirds of the mice use in this study (A^y/a: n = 10/14; a/a: n = 4/8). Due to the yellow coat color of the mice with the A^y allele, we can be confident in the mouse genotype; however, directly evaluating the glycemic control to the extent of tissue material changes was not possible for every mouse. Second, the lack of double-labels for bone formation prevented identification of the mechanism responsible for the changes in the observed tissue properties. In particular, because onset of T2DM in the A^y/a mice occurred prior to attainment of skeletal maturity, the contribution of any differences in periosteal expansion and endosteal resorption between groups to the observed compositional differences could not be assessed. Third, the small masses of metaphyseal trabecular tissue and diaphyseal cortical tissue in these specimens precluded separate HPLC analyses of trabecular and cortical bone, and the whole proximal femurs were homogenized. Thus, the crosslinks measured by HPLC are a mixture of both cortical and trabecular crosslinks. Because the proximal femurs were mostly cortical bone by mass (exemplified in Figs. 1*B*, 1*D*, 2*A*, and 2*B*), it is likely that the measured pentosidine concentration was dominated by pentosidine from cortical tissue. On the other hand, a negligible contribution of pentosidine from trabecular tissue cannot be guaranteed. The inability to differentiate pentosidine concentrations in the trabecular and cortical compartments is a major limitation of this assay because AGEs differentially accumulate in a compartment-dependent manner.[49,50,52,53] However, the HPLC analysis of the homogenized tissue provides insight into collagen crosslinking at the level of the whole proximal femur, and the results of these analyses can be directly compared to the whole-proximal-femur region FTIR parameters. Last, we note that the concentrations of HP and LP found in our study are slightly higher than previously reported values[55]; however, our ratio of HP to LP is well within established ranges.[55] Although the femurs were carefully cleaned of soft tissue prior to hydrolysis for HPLC analysis, it is possible that small contributions of soft tissue were included in the HPLC collagen crosslink assessments, which could increase HP and LP concentrations.[55] Nevertheless, the data presented here contribute to the understanding of bone material property changes in T2DM due to hyperglycemia.

Author Manuscript Author Manuscript Author Manuscript Author Manuscript

This work is the first to characterize the compositional characteristics of bone in the KK-Ay mouse. Our study showed spatially-resolved changes in tissue-level material properties due to hyperglycemia in the KK-Ay mouse, and the findings of increased mean collagen maturity and mineral content in the KK-Ay mice compared to controls is consistent with previous documentation of reduced bone turnover with T2DM. Overt T2DM manifests in KK-Ay mice around 8 weeks of age as a result of insulin resistance, thus the KK-Ay mouse exhibits an essential feature of T2DM in humans. In summary, the observed changes in the tissue material properties of KK-Ay mice contribute to an evolving understanding of alterations in bone quality with T2DM.

Supplementary Material

Refer to Web version on PubMed Central for supplementary material.

Acknowledgments

The FTIR and HPLC work was supported by NIH National Institute of Arthritis and Musculoskeletal and Skin Diseases (NIAMS) K01AR064314 (to ED), National Science Foundation Graduate Research Fellowship Program (NSF DGE) DGE-1144153 (to HBH), and Cornell Engineering Learning Initiatives (to DRD). The animal study was supported by the Orthopaedic Research and Education Foundation Goldberg Arthritis Research Grant (to KBK). We thank Michele Chin, Tarryn Tertulien, Daniel Weinreb, Ida Adjivon, and Rena Mazur for assistance with FTIR data collection; Ashley Lloyd for support with the mixed effects modeling; William Schroeder and Ryan Clark for animal care; and Eleftherios Paschalis for assistance with data interpretation.

Authors' roles: Study design: ED and KBK. Study conduct: HBH, JCP, DRD, KBK, and ED. Data collection: HBH, JCP, and DRD. Data analysis: HBH and JCP. Data interpretation: HBH, KBK, and ED. Drafting manuscript: HBH and ED. Revising manuscript content: HBH, JCP, KBK, and ED. Approving final version of manuscript: HBH, JCP, DRD, KBK, and ED. Integrity of data analysis: HBH, ED.

References

1. de Liefde II, van der Klift M, de Laet CE, van Daele PL, Hofman A, Pols HA. Bone mineral density and fracture risk in type-2 diabetes mellitus: The Rotterdam Study. Osteoporos Int. 2005; 16:1713–20. [PubMed: 15940395]
2. Schwartz AV, Vittinghoff E, Bauer DC, et al. Study of Osteoporotic Fractures (SOF) Research Group; Osteoporotic Fractures in Men (MrOS) Research Group; Health, Aging, and Body Composition (Health ABC) Research Group. Association of BMD and FRAX score with risk of fracture in older adults with type 2 diabetes. JAMA. 2011; 305(21):2184–92. [PubMed: 21632482]
3. Janghorbani M, Van Dam RM, Willett WC, Hu FB. Systematic review of type 1 and type 2 diabetes mellitus and risk of fracture. Am J Epidemiol. 2007; 166:495–505. [PubMed: 17575306]
4. Eyre DR, Weis MA, Wu JJ. Advances in collagen cross-link analysis. Methods. 2008; 45:65–74. [PubMed: 18442706]
5. Avery NC, Bailey AJ. Enzymic and non-enzymic cross-linking mechanisms in relation to turnover of collagen: relevance to aging and exercise. Scand J Med Sci Sport. 2005; 15:231–40.
6. Oxlund H, Barckman M, Ørtoft G, Andreassen TT. Reduced concentrations of collagen cross-links are associated with reduced strength of bone. Bone. 1995; 17:365S–71S. [PubMed: 8579939]
7. Nyman JS. Effect of diabetes on the fracture resistance of bone. Clin Rev Bone Miner Metab. 2013; 11:38–48.
8. Tang SY, Vashishth D. The relative contributions of non-enzymatic glycation and cortical porosity on the fracture toughness of aging bone. J Biomech. 2011; 44:330–6. [PubMed: 21056419]
9. Vashishth D, Gibson GJ, Khoury JI, et al. Influence of nonenzymatic glycation on biomechanical properties of cortical bone. Bone. 2001; 28:195–201. [PubMed: 11182378]

Author Manuscript Author Manuscript Author Manuscript Author Manuscript

10. Nyman JS, Even JL, Jo CH, et al. Increasing duration of type 1 diabetes perturbs the strength-structure relationship and increases brittleness of bone. Bone. 2011; 48:733–40. [PubMed: 21185416]
11. Saito M, Fujii K, Mori Y, Marumo K. Role of collagen enzymatic and glycation induced cross-links as a determinant of bone quality in spontaneously diabetic WBN/Kob rats. Osteoporos Int. 2006; 17:1514–23. [PubMed: 16770520]
12. McCarthy AD, Etcheverry SB, Bruzzone L, et al. Non-enzymatic glycosylation of a type I collagen matrix: effects on osteoblastic development and oxidative stress. BMC Cell Biol. 2001; 2:16. [PubMed: 11518540]
13. Katayama Y, Akatsu T, Yamamoto M, Kugai N, Nagata N. Role of nonenzymatic glycosylation of type I collagen in diabetic osteopenia. J Bone Miner Res. 1996; 11:931–7. [PubMed: 8797113]
14. Mercer N, Ahmed H, Etcheverry SB, Vasta GR, Cortizo AM. Regulation of advanced glycation end product (AGE) receptors and apoptosis by AGEs in osteoblast-like cells. Mol Cell Biochem. 2007; 306:87–94. [PubMed: 17660952]
15. Krakauer JC, McKenna MJ, Buderer NF, et al. Bone loss and bone turnover in diabetes. Diabetes. 1995; 44:775–82. [PubMed: 7789645]
16. Pedrazzoni M, Ciotti G, Pioli G, et al. Osteocalcin levels in diabetic subjects. Calcif Tissue Int. 1989; 45:331–6. [PubMed: 2804765]
17. Shu A, Yin M, Stein E, et al. Bone structure and turnover in type 2 diabetes mellitus. Osteoporos Int. 2012; 23:635–41. [PubMed: 21424265]
18. Gerdhem P, Isaksson A, Åkesson K, Obrant KJ. Increased bone density and decreased bone turnover, but no evident alteration of fracture susceptibility in elderly women with diabetes mellitus. Osteoporos Int. 2005; 16:1506–12. [PubMed: 15824889]
19. Fajardo RJ, Karim L, Calley VI, Bouxsein ML. A review of rodent models of type 2 diabetic skeletal fragility. J Bone Miner Res. 2014; 29:1025–40. [PubMed: 24585709]
20. Nakamura M. A diabetic strain of the mouse. Proc Jpn Acad. 1962; 38:348–52.
21. Ikeda H. KK mouse. Diabetes Res Clin Pract. 1994; 24:S313–6. [PubMed: 7859626]
22. Iwatsuka H, Shino A, Suzuoki Z. General survey of diabetic features of yellow KK mice. Endocrinol Jpn. 1970; 17:23–35. [PubMed: 5468422]
23. Taketomi S, Tsuda M, Matsuo T, et al. Alterations of hepatic enzyme activities in KK and yellow KK mice with various diabetic states. Horm Metab Res. 1973; 5:333–9. [PubMed: 4148927]
24. Xu F, Dong Y, Huang X, et al. Decreased osteoclastogenesis, osteoblastogenesis and low bone mass in a mouse model of type 2 diabetes. Mol Med Rep. 2014; 10:1935–41. [PubMed: 25109926]
25. Fu C, Zhang X, Ye F, Yang J. High insulin levels in KK-Ay diabetic mice cause increased cortical bone mass and impaired trabecular micro-structure. Int J Mol Sci. 2015; 16:8213–26. [PubMed: 25872143]
26. Takagi S, Miura T, Yamashita T, et al. Characteristics of diabetic osteopenia in KK-Ay diabetic mice. Biol Pharm Bull. 2012; 4383:438–43.
27. Creecy A, Uppuganti S, Merkel AR, et al. Changes in the fracture resistance of bone with the progression of type 2 diabetes in the ZDSD rat. Calcif Tissue Int. 2016; 99:289–301. [PubMed: 27209312]
28. Pritchard JM, Papaioannou A, Schwarcz HP, et al. A comparison of collagen crosslink content in bone specimens from elective total hip arthroplasty patients with and without type 2 diabetes. J Bone Rep Recomm. 2016; 2:3.
29. Oren TW, Botolin S, Williams A, Bucknell A, King KB. Arthroplasty in veterans: analysis of cartilage, bone, serum, and synovial fluid reveals differences and similarities in osteoarthritis with and without comorbid diabetes. J Rehabil Res Dev. 2011; 48:1195–210. [PubMed: 22234664]
30. Prisby RD, Swift JM, Bloomfield SA, Hogan HA, Delp MD. Altered bone mass, geometry and mechanical properties during the development and progression of type 2 diabetes in the Zucker diabetic fatty rat. J Endocrinol. 2008; 199:379–88. [PubMed: 18755885]
31. Zhang L, Liu Y, Wang D, et al. Bone biomechanical and histomorphometrical investment in type 2 diabetic Goto-Kakizaki rats. Acta Diabetol. 2009; 46:119–26. [PubMed: 18843446]

Author Manuscript Author Manuscript Author Manuscript Author Manuscript

32. Hammond MA, Gallant MA, Burr DB, Wallace JM. Nanoscale changes in collagen are reflected in physical and mechanical properties of bone at the microscale in diabetic rats. Bone. 2014; 60:26–32. [PubMed: 24269519]
33. McNulty MM, Schroeder WG, Bucknell AJ, Rosenthal AK, King KB. Hyperglycemia increases incidence of osteophyte formation in a mouse model of osteoarthritis. Osteoarthritis Cartilage. 2015; 23:A286.
34. Glasson SS, Blanchet TJ, Morris EA. The surgical destabilization of the medial meniscus (DMM) model of osteoarthritis in the 129/SvEv mouse. Osteoarthritis Cartilage. 2007; 15:1061–9. [PubMed: 17470400]
35. Ayala JE, Samuel VT, Morton GJ, et al. Standard operating procedures for describing and performing metabolic tests of glucose homeostasis in mice. Dis Model Mech. 2010; 3:525–34. [PubMed: 20713647]
36. Gourion-Arsiquaud, S., West, PA., Boskey, AL. Fourier transform-infrared microspectroscopy and microscopic imaging. In: Westendorf, JJ., editor. Osteoporosis: methods and protocols. New York: Humana Press; 2008. p. 293-303.(Methods in Molecular Biology; vol. 455)
37. Boskey A, Mendelsohn R. Infrared analysis of bone in health and disease. J Biomed Opt. 2005; 10:31102.
38. Faibish D, Gomes A, Boivin G, Binderman I, Boskey A. Infrared imaging of calcified tissue in bone biopsies from adults with osteomalacia. Bone. 2005; 36:6–12. [PubMed: 15663997]
39. Taylor EA, Lloyd AA, Salazar-Lara C, Donnelly EL. Raman and Fourier transform infrared (FT-IR) mineral to matrix ratios correlate with physical chemical properties of model compounds and native bone tissue. Appl Spectrosc. 2017; 71(10):2404–10. [PubMed: 28485618]
40. Paschalis EP, Mayo WE, Boskey AL, Mendelsohn R. infrared microscopic imaging of bone: spatial. J Bone Miner Res. 2001; 16:893–900. [PubMed: 11341334]
41. Paschalis EP, Verdelis K, Doty SB, et al. Spectroscopic characterization of collagen cross-links in bone. J Bone Miner Res. 2001; 16:1821–8. [PubMed: 11585346]
42. Pleshko N, Boskey A, Mendelsohn R. Novel infrared spectroscopic method for the determination of crystallinity of hydroxyapatite minerals. Biophys J. 1991; 60:786–93. [PubMed: 1660314]
43. Bank RA, Beekman B, Verzijl N, et al. Sensitive fluorimetric quantitation of pyridinium and pentosidine crosslinks in biological samples in a single high-performance liquid chromatographic run. J Chromatogr B Biomed Appl. 1997; 703:37–44.
44. Bank RA, Jansen EJ, Beekman B, te Koppele JM. Amino acid analysis by reverse-phase high-performance liquid chromatography: improved derivatization and detection conditions with 9-fluorenylmethyl chloroformate. Anal Biochem. 1996; 240:167–76. [PubMed: 8811901]
45. Donnelly E, Boskey AL, Baker SP, van der Meulen MC. Effects of tissue age on bone tissue material composition and nanomechanical properties in the rat cortex. J Biomed Mater Res A. 2010; 92(3):1048–56. [PubMed: 19301272]
46. Donnelly E, Meredith DS, Nguyen JT, et al. Reduced cortical bone compositional heterogeneity with bisphosphonate treatment in postmenopausal women with intertrochanteric and subtrochanteric fractures. J Bone Miner Res. 2012; 27:672–8. [PubMed: 22072397]
47. Allen MR, Hock JM, Burr DB. Periosteum: biology, regulation, and response to osteoporosis therapies. Bone. 2004; 35:1003–12. [PubMed: 15542024]
48. Schaffler MB, Cheung WY, Majeska R, Kennedy O. Osteocytes: master orchestrators of bone. Calcif Tissue Int. 2014; 94:5–24. [PubMed: 24042263]
49. Sroga GE, Siddula A, Vashishth D. Glycation of human cortical and cancellous bone captures differences in the formation of Maillard reaction products between glucose and ribose. PLoS One. 2015; 10:1–19.
50. Karim L, Tang SY, Sroga GE, Vashishth D. Differences in non-enzymatic glycation and collagen cross-links between human cortical and cancellous bone. Osteoporos Int. 2013; 24:2441–7. [PubMed: 23471564]
51. Sell DR, Nagaraj RH, Grandhee SK, et al. Pentosidine: a molecular marker for the cumulative damage to proteins in diabetes, aging, and uremia. Diabetes Metab Rev. 1991; 7:239–51. [PubMed: 1813279]

Author Manuscript Author Manuscript Author Manuscript Author Manuscript

52. Farlay D, Armas LA, Gineyts E, Akhter MP, Recker RR, Boivin G. Nonenzymatic glycation and degree of mineralization are higher in bone from fractured patients with type 1 diabetes mellitus. J Bone Miner Res. 2016; 31:190–5. [PubMed: 26234180]

53. Odetti P, Rossi S, Monacelli F, et al. Advanced glycation end products and bone loss during aging. Ann N Y Acad Sci. 2005; 1043:710–7. [PubMed: 16037297]

54. Singh R, Barden A, Mori T, Beilin L. Advanced glycation end-products: a review. Diabetologia. 2001; 44:129–46. [PubMed: 11270668]

55. Eyre DR, Koob TJ, Van Ness KP. Quantitation of hydroxypyridinium crosslinks in collagen by high-performance liquid chromatography. Anal Biochem. 1984; 137:380–8. [PubMed: 6731820]

Author Manuscript Author Manuscript Author Manuscript Author Manuscript

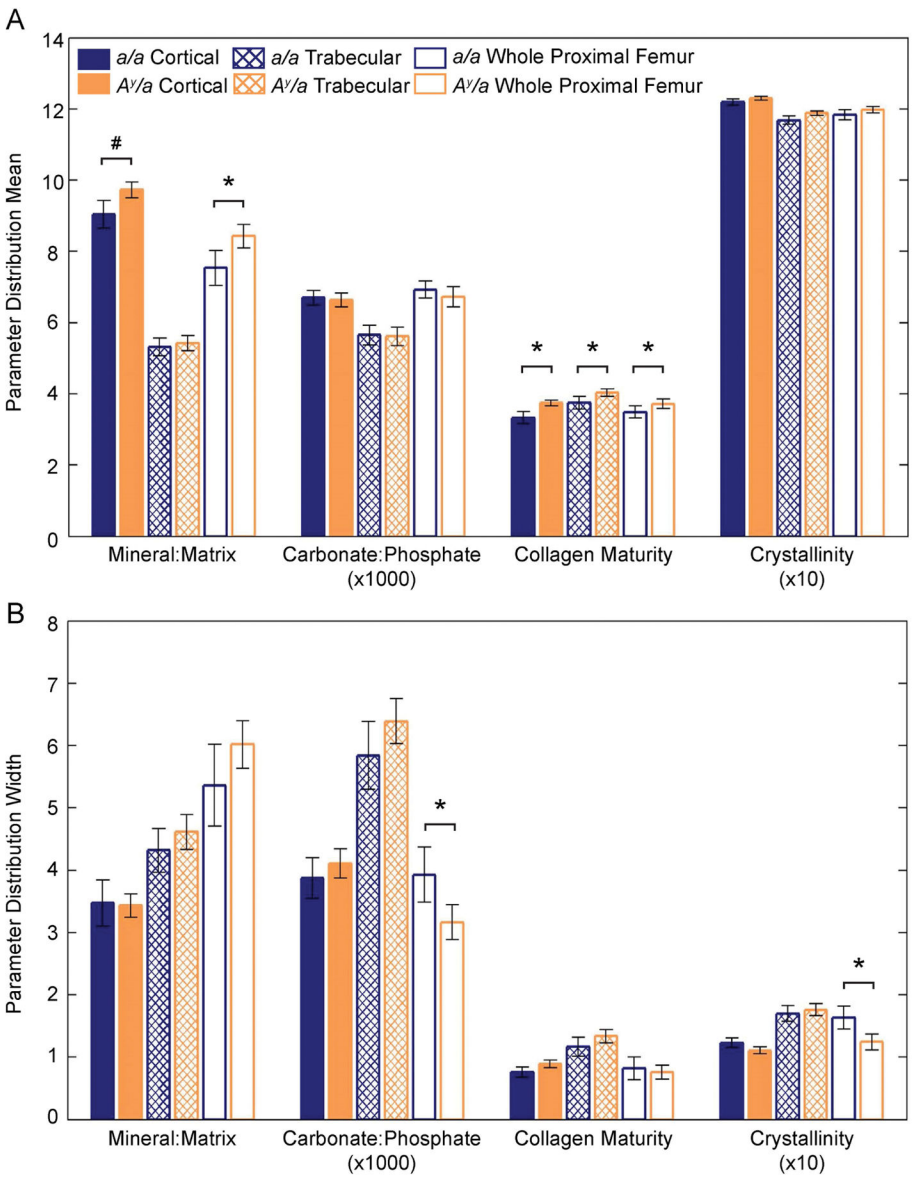

Fig. 1.

FTIR parameter distribution means (*A*) and widths (*B*) for cortical, trabecular, and whole-proximal-femur regions by group. Bar heights indicate the parameter means, and error bars denote the 95% confidence interval. *$p < 0.05$, #$p < 0.10$ after adjustment for repeated measures in the linear mixed models.

Author Manuscript Author Manuscript Author Manuscript Author Manuscript

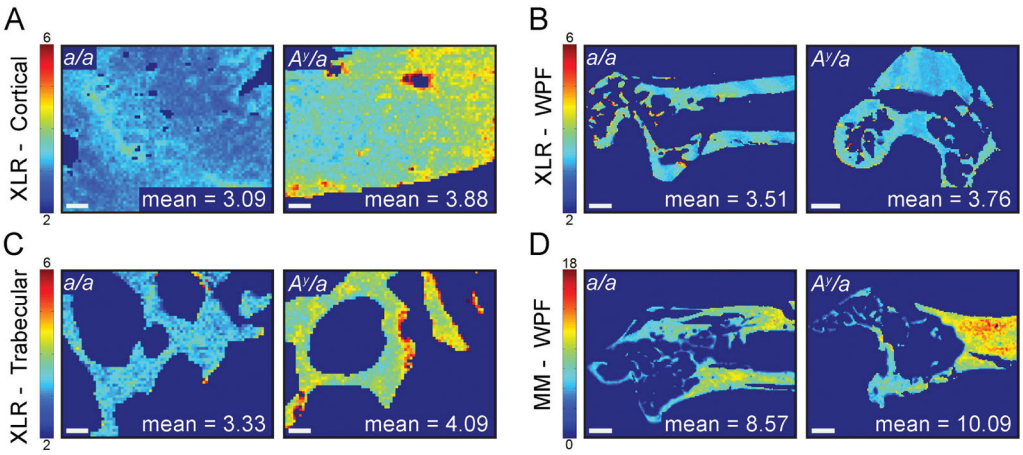

Fig. 2.

Representative images of selected FTIR parameters in *a/a* and *A^Y^/a* mouse bone for (*A*) cortical collagen maturity, (*B*) whole proximal femur collagen maturity, (*C*) trabecular collagen maturity, and (*D*) whole proximal femur mineral:matrix ratio. Scale bars indicate 50 μm in cortical and trabecular images and 500 μm in whole-proximal-femur images.

Author Manuscript Author Manuscript Author Manuscript Author Manuscript

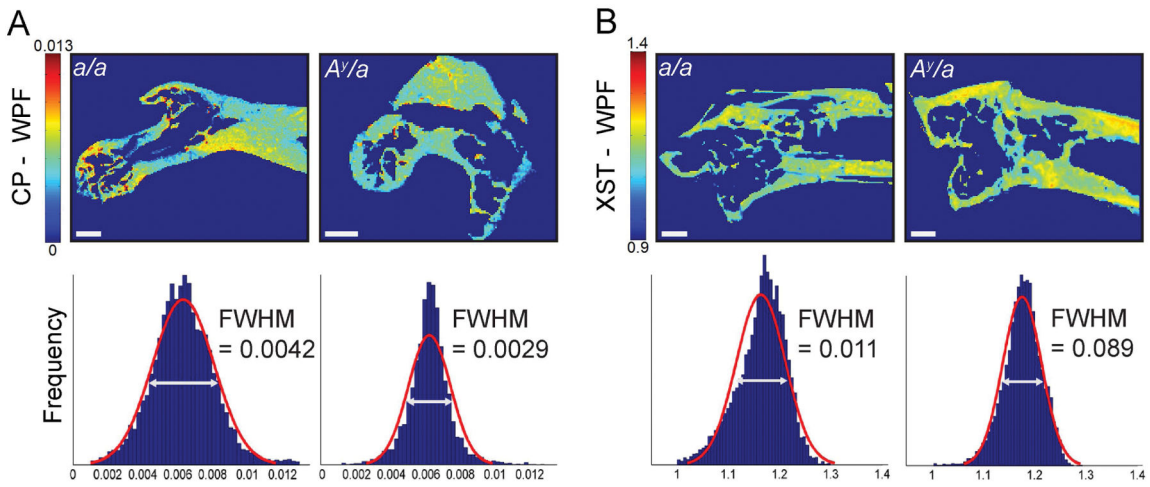

Fig. 3.

Representative images of selected FTIR parameters and corresponding pixel histograms in *a/a* and A^{y}/a specimens for (*A*) whole proximal femur carbonate:phosphate ratio, and (*B*) whole proximal femur crystallinity. Scale bars on FTIR images indicate 500 μm. The red curve on each pixel histograms indicates the Gaussian distribution fit, and the white horizontal bar with arrows indicates the FWHM. FWHM = full-width at half-maximum.

Author Manuscript

Author Manuscript

Author Manuscript

Author Manuscript

Table 1

Concentrations of Collagen Crosslinks Determined With HPLC and Selected Collagen Crosslink Ratios

Outcome	*a/a* (mean ± SD)	A^y/a (mean ± SD)	p^a
Pentosidine (mmol/mol collagen)	2.12 ± 1.04	2.48 ± 1.48	0.6300
HP (mol/mol collagen)	0.59 ± 0.30	0.68 ± 0.28	0.5586
LP (mol/mol collagen)	0.24 ± 0.09	0.24 ± 0.13	0.5380
HP:LP	2.50 ± 0.79	2.95 ± 0.83	0.8788
HP+LP	0.82 ± 0.36	2.42 ± 1.48	0.7055
Pentosidine:HP+LP	2.68 ± 1.00	2.75 ± 1.04	0.5597

HP = hydroxylysyl pyridinoline; LP = lysyl pyridinoline.

[a]Value of *p* represents Student's *t* test between A^y/a and *a/a* groups.

Author Manuscript Author Manuscript Author Manuscript Author Manuscript

Table 2

Correlations Between Lifetime-Average Blood Glucose and Pentosidine With FTIR Imaging Parameters and HPLC-Determined Collagen Crosslinks

	Lifetime-average blood glucose (mg/dL)			Pentosidine (mmol/mol collagen)		
Outcome	**Correlation coefficient (*r*)**	***R*²**	***p***	**Correlation coefficient (*r*)**	***R*²**	***p***
FTIR imaging						
Trabecular						
Mean collagen maturity	0.503	0.253	0.0669	N/A	N/A	N/A
Carbonate:phosphate ratio FWHM	0.626	0.392	**0.0166**	N/A	N/A	N/A
Collagen maturity FWHM	0.552	0.305	**0.0407**	N/A	N/A	N/A
Whole proximal femur						
Mean collagen maturity	0.600	0.361	**0.0300**	0.238	0.057	0.3116
Mineral:matrix ratio FWHM	0.568	0.322	0.0685	0.040	0.002	0.8755
Carbonate:phosphate ratio FWHM	−0.656	0.430	**0.0150**	0.048	0.002	0.8406
Crystallinity FWHM	−0.763	0.582	**0.0024**	0.032	0.001	0.8928
HPLC						
Pentosidine	0.233	0.054	0.4441	N/A	N/A	N/A
HP	0.242	0.059	0.3906	0.597	0.357	**0.0042**
LP	0.339	0.115	0.2573	0.877	0.769	**0.0006**
HP:LP	0.003	0.000	0.9931	0.241	0.058	0.2920
HP+LP	0.293	0.086	0.3312	0.715	0.511	**0.0003**
Pentosidine:HP+LP	0.166	0.027	0.5888	N/A	N/A	N/A

Bold values indicate $p < 0.05$.

FWHM = full-width at half-maximum; N/A = not applicable; HP = hydroxylysyl pyridinoline; LP = lysyl pyridinoline.